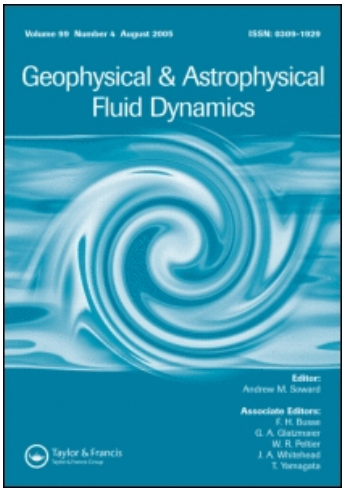

Geophysical & Astrophysical Fluid Dynamics
Publication details, including instructions for authors and subscription information:
http://www.informaworld.com/smpp/title~content=t713642804

Taylor's constraint in a spherical αω-dynamo

Rainer Hollerbach[ab]; Carlo F. Barenghi[a]; Chris A. Jones[ab]
[a] Department of Mathematics and Statistics, University of Newcastle upon Tyne, Newcastle Tyne, UK [b] Department of Mathematics, University of Exeter, Exeter, UK

To cite this Article Hollerbach, Rainer , Barenghi, Carlo F. and Jones, Chris A.(1992) 'Taylor's constraint in a spherical αω-dynamo', Geophysical & Astrophysical Fluid Dynamics, 67: 1, 3 — 25
To link to this Article: DOI: 10.1080/03091929208201834
URL: http://dx.doi.org/10.1080/03091929208201834

Geophys. Astrophys. Fluid Dynamics, Vol. 67, pp. 3–25
Reprints available directly from the publisher
Photocopying permitted by license only

TAYLOR'S CONSTRAINT IN A SPHERICAL $\alpha\omega$-DYNAMO

RAINER HOLLERBACH†, CARLO F. BARENGHI and CHRIS A. JONES†

Department of Mathematics and Statistics, University of Newcastle upon Tyne, Newcastle upon Tyne NE1 7RU UK

(*Received 9 October 1991; in final form December 20, 1991*)

The α^2-dynamo of Hollerbach and Ierley (1991) is converted into an $\alpha\omega$-dynamo, and the analysis of Barenghi and Jones (1991) is extended. Only one choice of α and ω is considered in detail, for both negative and positive dynamo numbers. The solutions in the viscously limited regime are qualitatively distinct, with negative D solutions oscillating about a zero mean, and positive D solutions oscillating about a non-zero mean. The existence of nonlinear eigenvalues D_x is demonstrated, beyond which the solutions are no longer viscously limited. The subsequent evolution would appear to be independent of the viscosity in some average sense, but there is no evidence of a true Taylor state.

KEY WORDS: $\alpha\omega$-dynamos, Taylor's constraint.

1. INTRODUCTION

In an earlier paper, Hollerbach and Ierley (1991), hereafter referred to as HI, we considered a modal α^2-dynamo in the limit of asymptotically small viscosity. In this paper we convert this α^2-dynamo into an $\alpha\omega$-dynamo, and again investigate the effect of Taylor's constraint in the limit of small viscosity. Although the details of the conversion from α^2 to $\alpha\omega$ are quite trivial, the subsequent evolution of the $\alpha\omega$-dynamo is unfortunately considerably more complicated.

Briefly, for the α^2-dynamos of HI, we found that as one increases the strength of the forcing beyond the linear critical eigenvalue α_c, the solutions remain viscously controlled, of order $\varepsilon^{1/2}$ (see 2.1), until a second critical eigenvalue α_T is reached, at which point Taylor's constraint is satisfied and the solutions become independent of the viscosity, of order one. There is thus a very clear distinction between the viscously limited regime and the Taylor regime. Furthermore, α^2 solutions are typically steady-state, making them particularly amenable to a detailed investigation.

In contrast, for the $\alpha\omega$-dynamo presented here, as one increases the strength of the forcing beyond the linear critical eigenvalue D_c, the solutions again remain viscously controlled until a second critical eigenvalue D_x is reached. Beyond D_x, however, the solutions are not unambiguously independent of the viscosity. $\alpha\omega$ solutions are typically oscillatory from the outset, and one is thus faced with the possibility that for parts of the evolution, Taylor's constraint is satisfied, but for other parts viscosity continues to play an essential role. One is thus neither in a true viscously limited regime nor in a true Taylor regime.

† Current address: Department of Mathematics, University of Exeter, North Park Road, Exeter EX4 4RE, UK.

Since the prospects of sorting out such a complicated evolution are rather daunting, only one choice of α and ω is investigated in detail, namely $\alpha = \alpha_0 \cos\theta$ and $\omega = \omega_0 r$. The kinematic eigenvalues of this particular model have been computed by Roberts (1972), and the viscously limited regime has been explored by Barenghi and Jones (1991), hereafter referred to as BJ, in a spherical shell. We duplicate the BJ results, and extend their analysis into the subsequent more complicated regime. Also, we consider both negative and positive dynamo numbers D; the solutions turn out to be qualitatively quite distinct, with negative D solutions oscillating about a zero mean, but positive D solutions oscillating about a non-zero mean. Various other choices of α and ω were also considered briefly, and indicate that the results reported here are the typical behaviour.

The next section presents the details of the conversion of HI to an $\alpha\omega$-dynamo. Sections 3 and 4 investigate, respectively, the solutions for negative and positive dynamo numbers, in each case starting with the viscously limited regime and proceeding to the more complicated subsequent evolution. Section 5 summarizes the main results and discusses some possible implications for the geodynamo problem.

2. MODAL AMPLITUDE EQUATIONS

The modal amplitude equations of HI are:

$$\frac{da_i}{dt} = -\lambda_{a_i}^2 a_i + \alpha_0 C_{ij}^{(1)} b_j + C_{ijkl}^{(4)} a_j a_k b_l, \tag{2.1a}$$

$$\frac{db_i}{dt} = -\lambda_{b_i}^2 b_i + \alpha_0 C_{ij}^{(2)} a_j + \varepsilon^{-1} C_{ijkl}^{(3)} a_j b_k a_l + C_{ijkl}^{(5)} b_j a_k b_l + C_{ijkl}^{(6)} a_j a_k a_l. \tag{2.1b}$$

To convert (2.1) to an $\alpha\omega$-dynamo, we begin by considering some kinematically prescribed differential rotation $v = \omega(r,\theta) r \sin\theta$ acting upon the magnetic field (in addition to the large-scale flow induced by the Lorentz force). From the induction equation [(2.5) of HI], its effect on the field will be to add a term

$$\frac{\partial B}{\partial t} = \ldots + M[\omega(r,\theta) r \sin\theta, A] \tag{2.2}$$

and following the subsequent development of HI this will add a term

$$\frac{db_i}{dt} = \ldots + \omega_0 C_{ij}^{(7)} a_j \tag{2.3}$$

to the amplitude equations (2.1), where ω_0 is the strength of the prescribed differential rotation, and its spatial structure is subsumed into the coefficient matrix $C^{(7)}$.

Now, we rescale (2.1) and (2.3) according to

$$\omega_0 = R_\omega \omega_0', \qquad \alpha_0 = R_\omega^{-1} \alpha_0',$$

$$a = R_\omega^{-1/2} a', \qquad b = R_\omega^{1/2} b', \tag{2.4}$$

$$\varepsilon = R_\omega^{-1} \varepsilon',$$

where R_ω is a magnetic Reynolds number based on this differential rotation, and is assumed to be large. This rescaling is incidentally the motivation for studying $\alpha\omega$-dynamos in the geophysical context, where the differential rotation is believed to be strong and the α-effect is consequently allowed to be weak. Note also that the (unobservable) toroidal field $B\hat{\mathbf{e}}_\phi$ is thus anticipated to be considerably stronger than the poloidal field $\nabla \times (A\hat{\mathbf{e}}_\phi)$. Finally, note that even though $\varepsilon' = R_\omega \varepsilon$, with R_ω large, one is still interested in the limit of small ε'.

So, dropping the primes, and neglecting two terms of relative order R_ω^{-2}, the rescaled equations are

$$\frac{da_i}{dt} = -\lambda_{a_i}^2 a_i + \alpha_0 C_{ij}^{(1)} b_j + C_{ijkl}^{(4)} a_j a_k b_l, \tag{2.5a}$$

$$\frac{db_i}{dt} = -\lambda_{b_i}^2 b_i + \omega_0 C_{ij}^{(7)} a_j + \varepsilon^{-1} C_{ijkl}^{(3)} a_j b_k a_l + C_{ijkl}^{(5)} b_j a_k b_l, \tag{2.5b}$$

and this completes the conversion to an $\alpha\omega$-dynamo. Essentially all we have done is regenerate B by an ω-effect rather than by an α-effect, and dropped one of the nonlinear terms. Even though a and b in (2.5) are no longer the same as in (2.1), the various coefficient arrays very conveniently are, with the exception of the new term in $C^{(7)}$, representing the prescribed differential rotation.

Note also that, having dropped the two $O(R_\omega^{-2})$ terms, (2.5) are invariant under a further rescaling of the form (2.4), and so there are only two independent parameters in (2.5), the dynamo number $D = \alpha_0 \omega_0$, measuring the strength of the total forcing, and ε, measuring the (rescaled) viscosity. For convenience, we take $\omega_0 = \pm 100$, and adjust the magnitude of D by adjusting α_0. (Strictly speaking, it is not quite accurate to say that the forcing is measured only by the product $\alpha_0 \omega_0$: Since (2.4) only applies for positive R_ω, one cannot change the signs of α_0 and ω_0 by this rescaling, and so $D = (+\alpha_0)(+\omega_0)$ is not equivalent to $D = (-\alpha_0)(-\omega_0)$. However, in the geophysical context α is generally taken to be positive in the northern hemisphere, and this eliminates the ambiguity in sign.)

The system of modal amplitude equations (2.5) is solved for pure dipole solutions, truncated at a total of 36 modes, 21 in A and 15 in B. In HI as few as 16 modes were sufficient to obtain a qualitative picture of the α^2 solutions, but the $\alpha\omega$ solutions exhibit greater spatial structure and thus require more modes. For the viscously limited solutions (incorporating $C^{(3)}$ as the only nonlinearity) a few runs were also

done with 49 modes, and clearly indicate that 36 modes are sufficient to obtain a qualitative picture. However, for the full system 49 modes would require the numerical evaluation and storage of far too many coefficients, and so the effect of the level of truncation on the full system is untested. Nevertheless, in view of the adequate resolution for the viscously limited solutions, and in view of the excellent agreement of the latter with the BJ model at a considerably higher truncation, it is at least plausible that the full system is also adequately resolved by 36 modes. See also Jones and Wallace (1992), who investigate a similar system in a duct geometry, and find similar dynamical behavior. Finally, it is worth mentioning, as pointed out by a referee of Hollerbach (1991), that at this resolution the possibility of achieving solutions of Braginsky's (1975, 1978) model-Z type is excluded *a priori*, since one could not hope to resolve the magnetic boundary layers that play such an essential role in model-Z.

3. $D<0$

We begin by considering the viscously limited regime, incorporating only the geostrophic nonlinearity $C^{(3)}$ in (2.5). For 36 modes the linear critical dynamo number is $D_c = -5513$, in agreement with Roberts' value of -5534. The resulting solutions are oscillatory, about a zero mean. Figure 1 shows a measure of the amplitude of

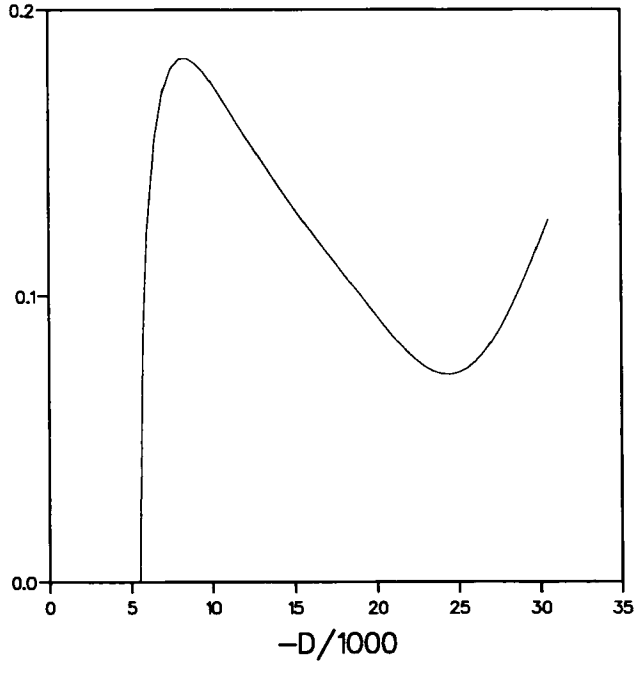

Figure 1 The amplitude of the viscously limited oscillation, measured as $(a_{1\max} b_{1\max})^{1/2}$, as a function of the (negative) dynamo number.

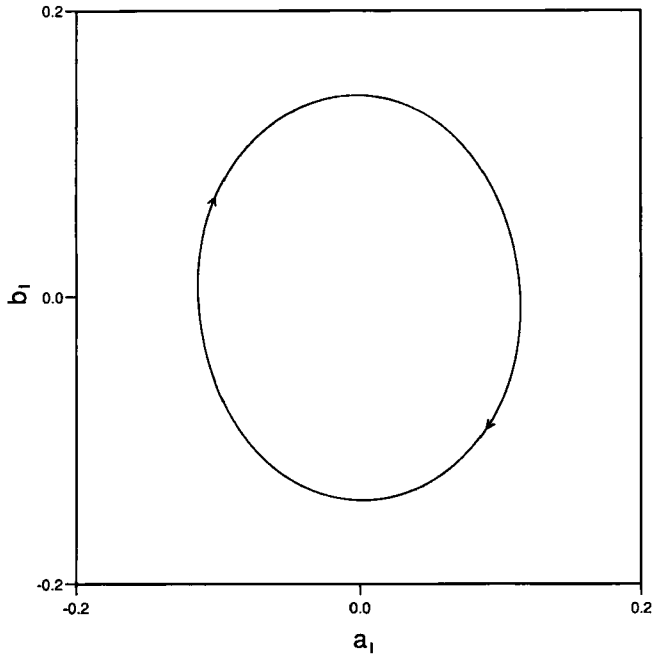

Figure 2 The trajectory in the phase space of b_1 versus a_1 for $D=-30600$. The period of the evolution is $T=0.045$.

the oscillation as one increases the magnitude of D. Figure 2 shows the trajectory in the phase space of b_1 versus a_1 for $D=-30600$. Note how remarkably simple the temporal evolution is, even at this considerable supercriticality. Figures 3 and 4 show the corresponding spatial structure of the fields; note the dynamo waves propagating from the pole to the equator.

However, if one now increases the magnitude to $D=-30800$, this simple evolution becomes unstable. Figure 5 shows the trajectory in phase space. Since this is a rather messy picture, Figure 6 shows a Poincaré section of the trajectory, strobed when $b_2=0$. The previously stable solution, consisting of just two points, is now unstable, and spirals outward in this rather elegant pattern. Furthermore, these spirals ultimately diverge to infinity; they do not settle down to a torus solution. So, beyond $D_x\approx -30700$, the geostrophic nonlinearity alone is no longer capable of equilibrating the field. This much is in exact agreement with the results of BJ.

Beyond D_x, we need to include the ageostrophic nonlinearities to equilibrate the field. Figures 7 and 8 show, respectively, the Poincaré sections of the trajectories for $D=-31750, \varepsilon^{-1}=100$ and $D=-31000, \varepsilon^{-1}=200$. One now has quasi-periodic torus solutions. Also shown for comparison are the two points each comprising the Poincaré sections of the singly-periodic viscously limited solutions, which turn out to be stabilized somewhat beyond D_x by the inclusion of the ageostrophic nonlinearities.

The ε-dependence of the quasi-periodic solutions is clearly more complicated than that of the singly-periodic solutions, which do indeed scale almost exactly as $\varepsilon^{1/2}$.

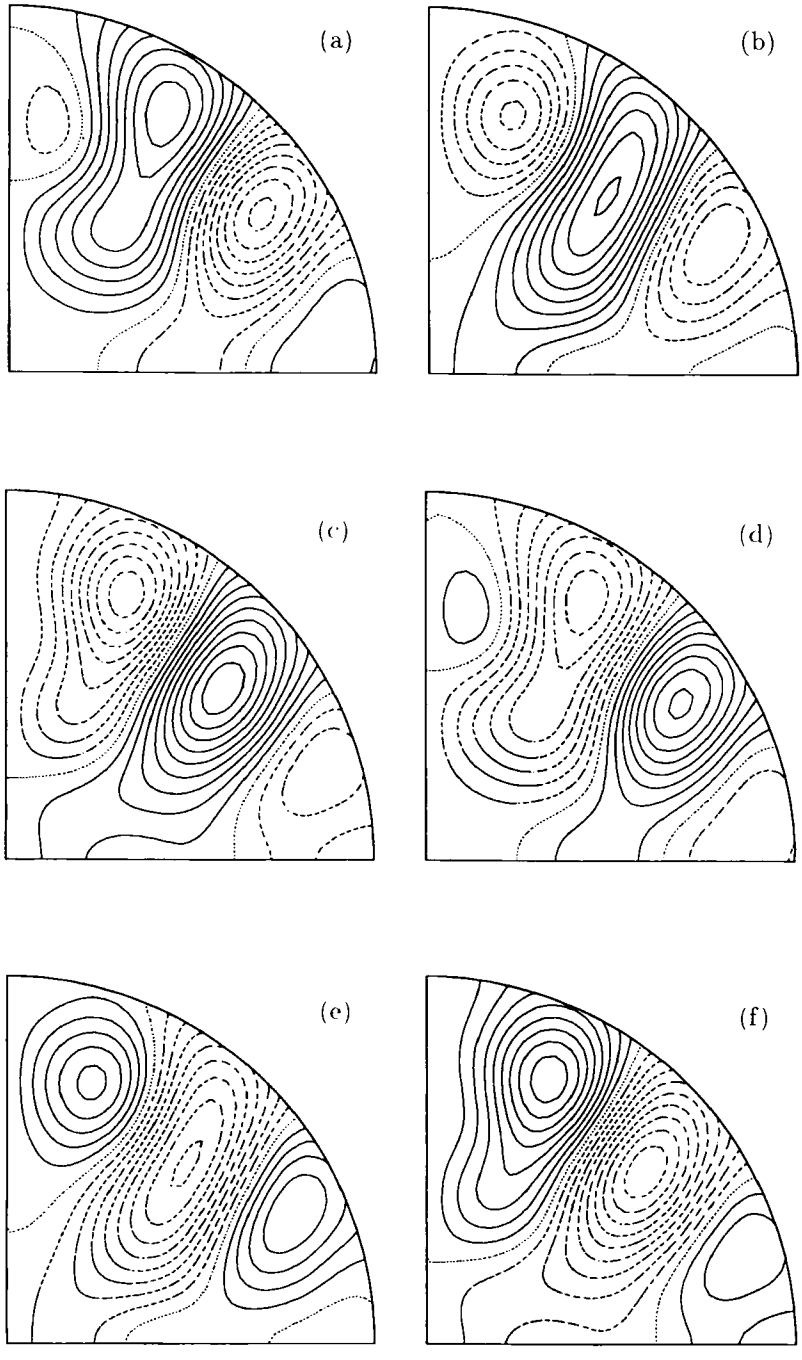

Figure 3 The spatial structure of A for $D = -30600$ through one period. (a) $t = (1/6)T$, (b) $t = (2/6)T$, (c) $t = (3/6)T$, (d) $t = (4/6)T$, (e) $t = (5/6)T$, (f) $t = (6/6)T$.

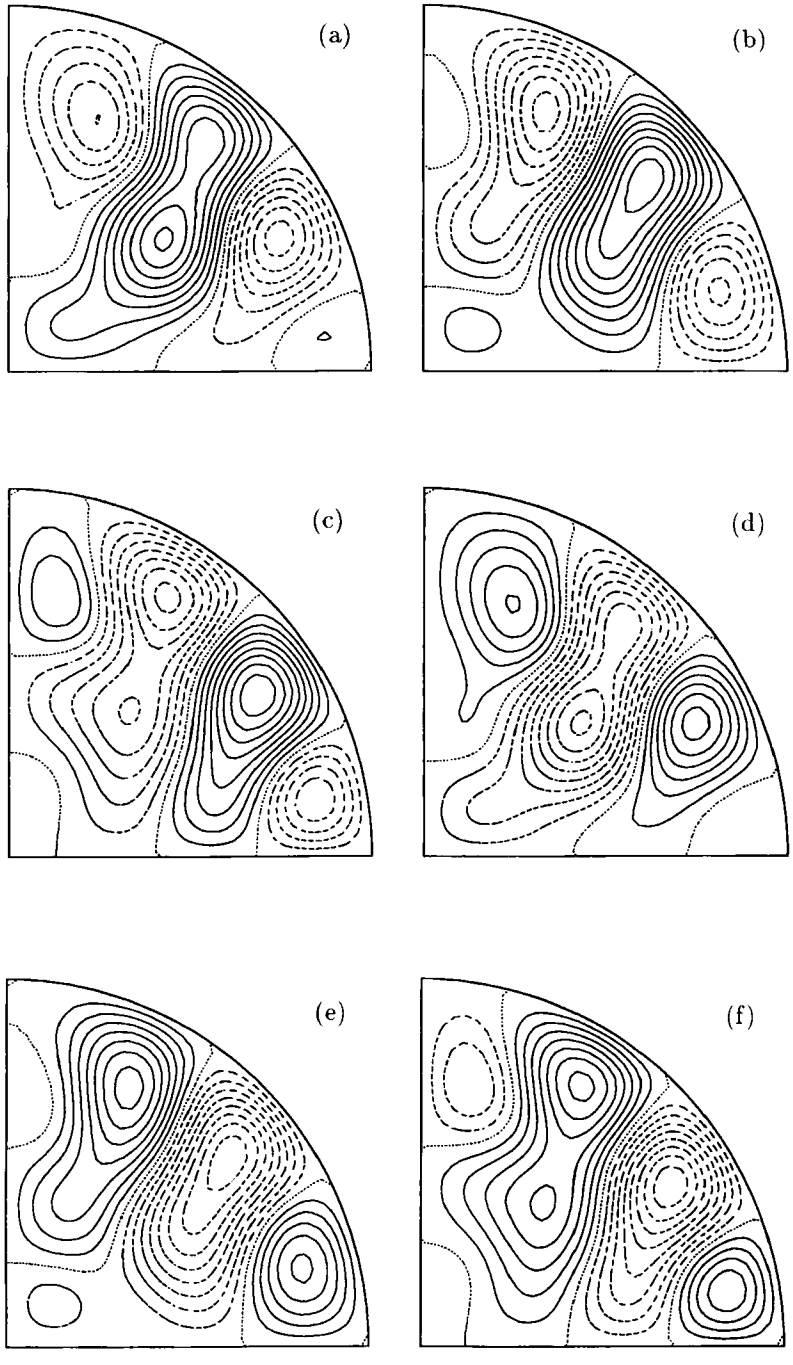

Figure 4 The spatial structure of B for $D=-30600$ through one period. (a) $t=(1/6)T$, (b) $t=(2/6)T$, (c) $t=(3/6)T$, (d) $t=(4/6)T$, (e) $t=(5/6)T$, (f) $t=(6/6)T$.

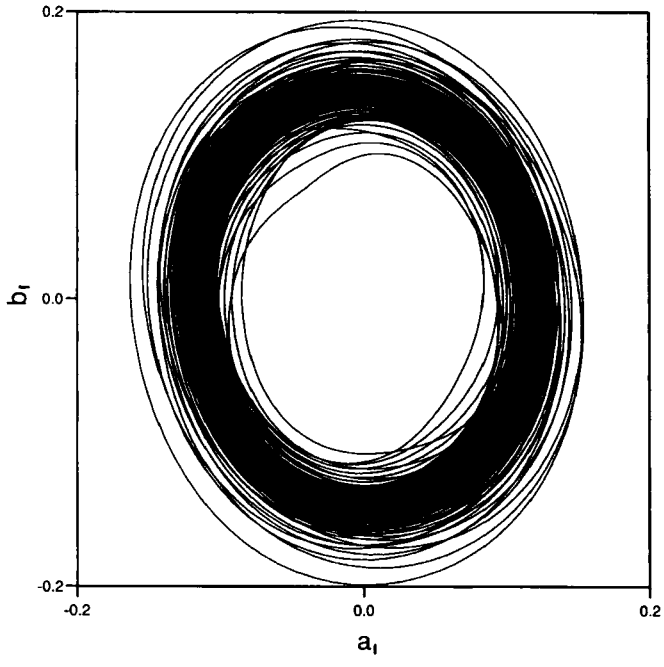

Figure 5 The trajectory in the phase space of b_1 versus a_1 for $D = -30800$.

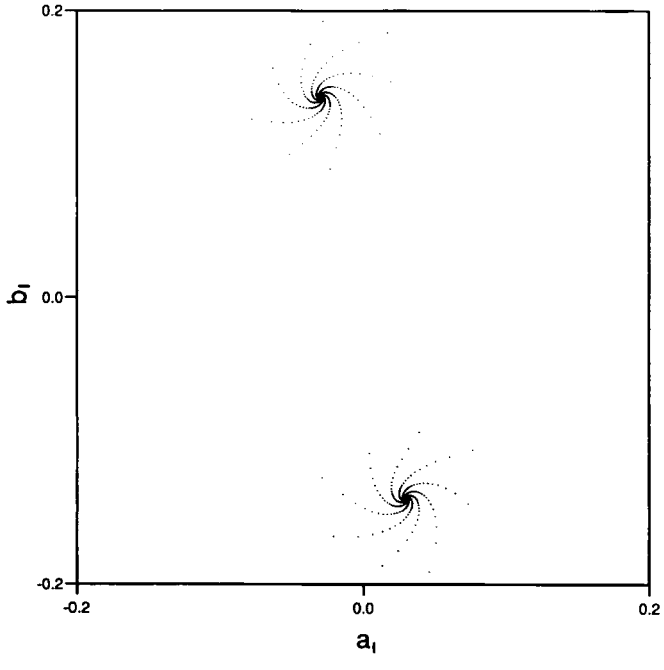

Figure 6 The Poincaré section of the trajectory in Figure 5, strobed when $b_2 = 0$.

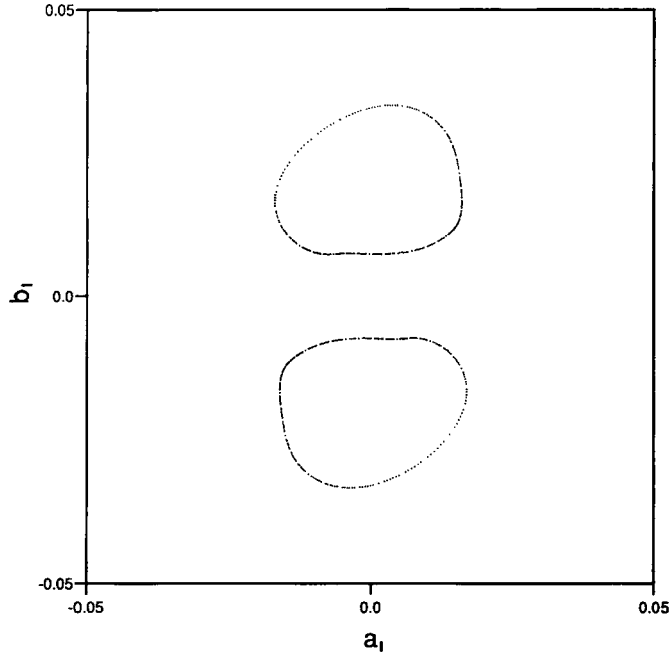

Figure 7 The Poincaré sections of the two possible solutions for $D = -31750$, $\varepsilon^{-1} = 100$.

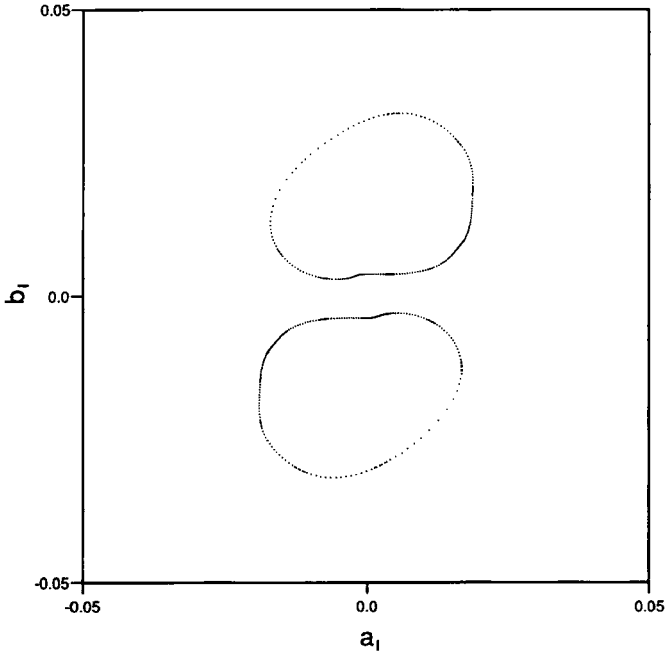

Figure 8 The Poincaré sections of the two possible solutions for $D = -31000$, $\varepsilon^{-1} = 200$.

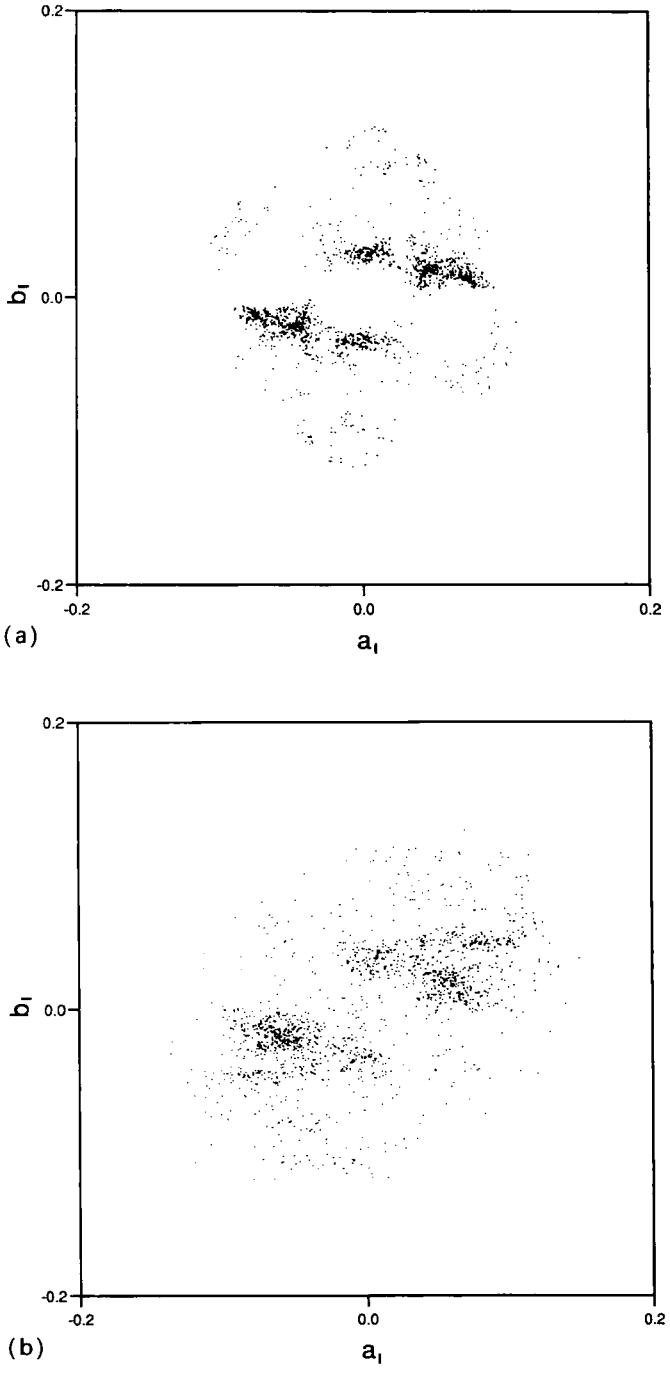

Figure 9 Two Poincaré sections for $D = -40000$. (a) $\varepsilon^{-1} = 100$, (b) $\varepsilon^{-1} = 200$. Each trajectory was run for 30 units of time, after allowing for the decay of transients.

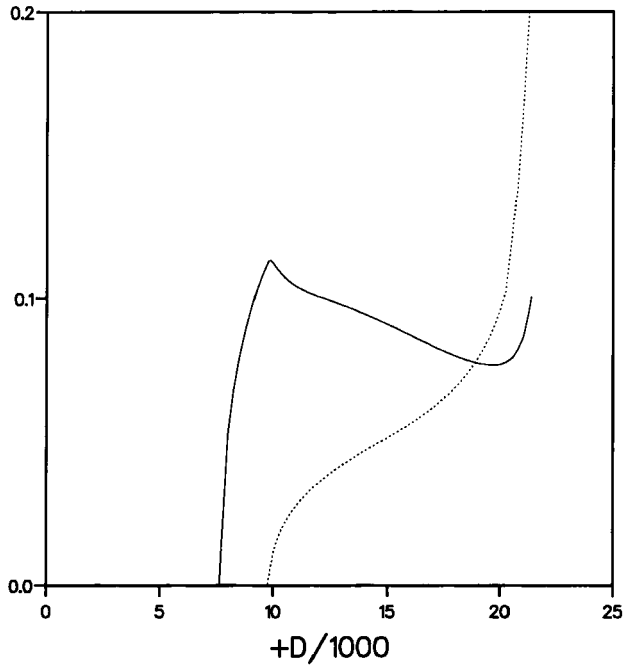

Figure 10 The amplitude of the viscously limited oscillation, measured as $\frac{1}{2}[(a_{1\max}-a_{1\min})(b_{1\max}-b_{1\min})]^{1/2}$, as a function of the (positive) dynamo number. Also, dashed, the offset from zero of the oscillation, measured as $(a_{1\max}+a_{1\min})/10$.

The outer portions of the torus appear to be almost independent of ε, whereas the inner portions appear to scale as ε. This would suggest that for parts of the temporal evolution Taylor's constraint is satisfied, but for other parts viscosity continues to play an essential role.

Of course, the issue is complicated by the fact that the two values $\varepsilon^{-1}=100$, 200 are hardly sufficient to establish the pattern in the asymptotic limit. Also—a reflection of the fact that one is not quite in the asymptotic limit—it is difficult to compare solutions at exactly the same dynamo numbers, since the secondary transitions of the torus solutions, discussed next, do not occur at exactly the same dynamo numbers for different values of ε. It is unfortunately not possible to investigate the true asymptotic limit, since the amplitude equations are extremely stiff, and one must reduce ones time-step when one reduces ε.

If one now increases the magnitude of D, these torus solutions develop further structure, evidently a transition to chaos interspersed with windows of phase-locking. The precise details are not investigated. Jumping instead to the fully chaotic regime at $D=-40000$, Figure 9 shows the two Poincaré sections for $\varepsilon^{-1}=100$, 200. Again, one notes that the pattern is sufficiently different that one would not want to claim the existence of a Taylor state. On the other hand, the average amplitude is not viscously limited, either.

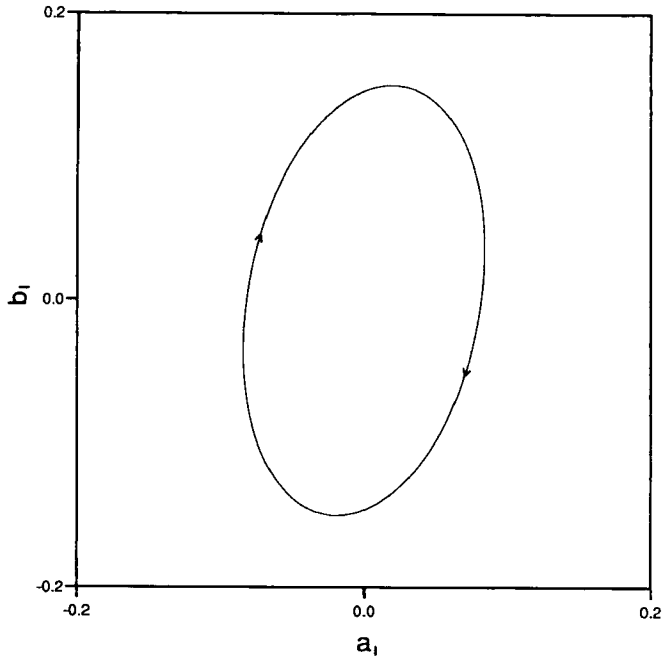

Figure 11 The trajectory in the phase space of b_1 versus a_1 for $D=9750$. The period of the evolution is $T=0.085$.

4. $D>0$

We again begin by considering the viscously limited regime, incorporating only the geostrophic nonlinearity $C^{(3)}$ in (2.5). For 36 modes the linear critical dynamo number is now $D_c=7621$, in agreement with Roberts' value of 7592. The resulting solutions are again oscillatory, about a zero mean. The solid line in Figure 10 shows a measure of the amplitude of the oscillation as one increases D. Figure 11 shows the trajectory in phase space for $D=9750$. Figures 12 and 13 show the corresponding spatial structure of the fields; note the dynamo waves propagating from the equator to the pole.

However, if one now increases D beyond $D_s\approx 9800$, a symmetry-breaking bifurcation occurs, and the solutions are now oscillatory about a non-zero mean. The dashed line in Figure 10 shows a measure of the offset from zero of the oscillation as one increases D. Figure 14 shows the two possible trajectories in phase space for $D=20000$. Figures 15 and 16 show the corresponding spatial structure of the fields; note the dynamo waves propagating from the equator to the pole in the outer regions, but the relatively stationary inner region. These results have been confirmed by the BJ model (unpublished).

One notes in Figure 10 that beyond $D_x\approx 21400$ the geostrophic nonlinearity alone is no longer capable of equilibrating the field, and so once again we need to include the ageostrophic nonlinearities. Figures 17 and 18 show, respectively, the two possible

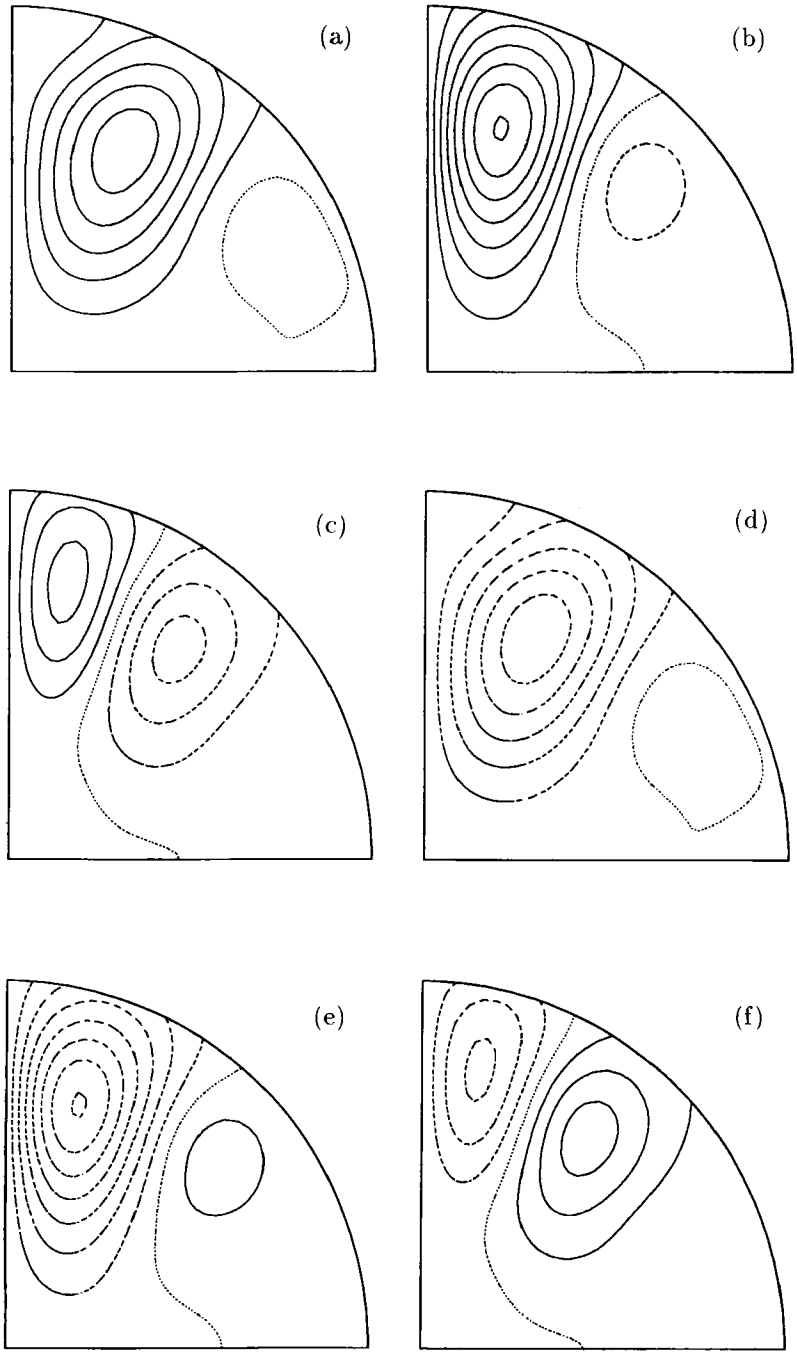

Figure 12 The spatial structure of A for $D=9750$ through one period. (a) $t=(1/6)T$, (b) $t=(2/6)T$, (c) $t=(3/6)T$, (d) $t=(4/6)T$, (e) $t=(5/6)T$, (f) $t=(6/6)T$.

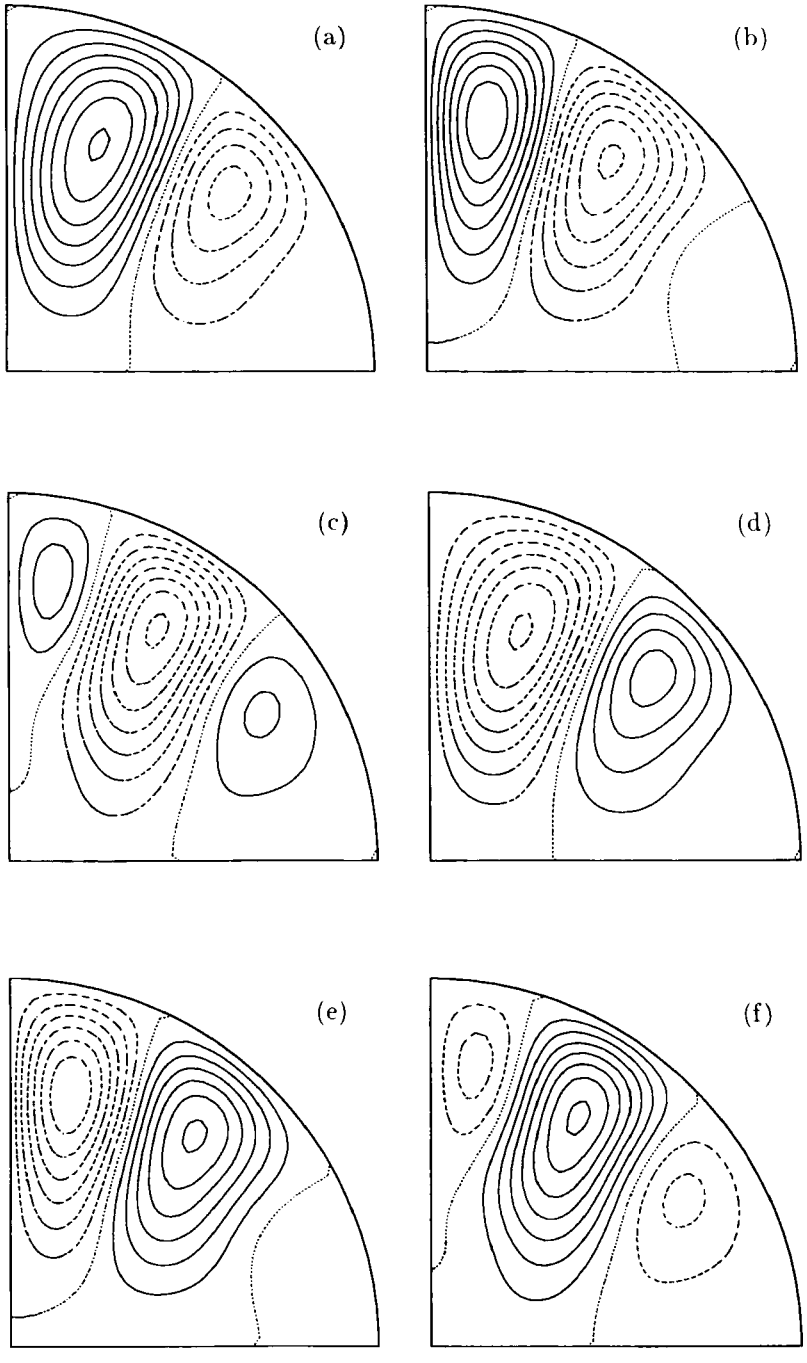

Figure 13 The spatial structure of B for $D=9750$ through one period. (a) $t=(1/6)T$, (b) $t=(2/6)T$, (c) $t=(3/6)T$, (d) $t=(4/6)T$, (e) $t=(5/6)T$, (f) $t=(6/6)T$.

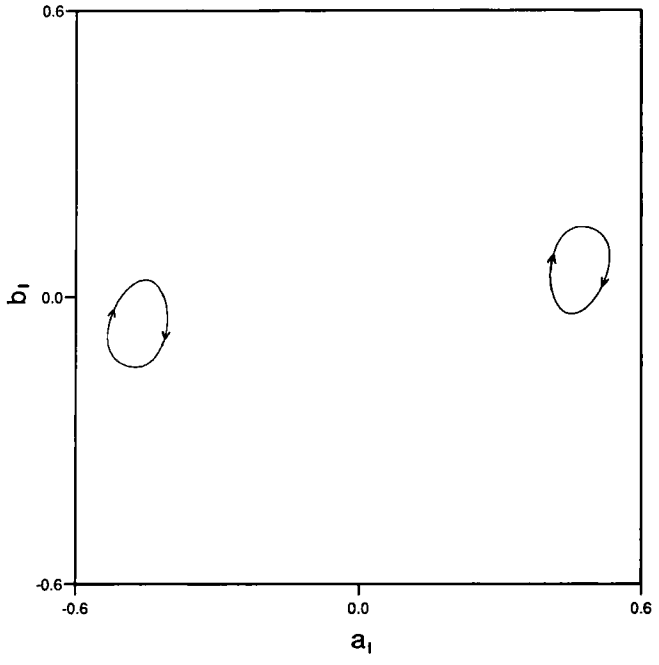

Figure 14 The two trajectories in the phase space of b_1 versus a_1 for $D=20000$. The period of the evolution is $T=0.054$.

trajectories each for $D=23000$, $\varepsilon^{-1}=100$ and $D=23200$, $\varepsilon^{-1}=200$. They are again quasi-periodic torus solutions, and the nature of the ε-dependence is again not clear.

If one now increases D, these torus solutions quickly break down and become chaotic. Furthermore, the two possible polarities coalesce to form a single chaotic trajectory. Jumping once again to the fully chaotic regime at $D=25000$, Figure 19 shows two typical trajectories for $\varepsilon^{-1}=100$, 200, and Figure 20 shows corresponding Poincaré sections for a considerably longer run. And again, one would not want to claim the existence of a Taylor state, but the average amplitude is not viscously limited, either.

5. DISCUSSION

The bifurcation diagram for negative and positive dynamo numbers is evidently as sketched in Figure 21. Up to D_x the geostrophic nonlinearity alone is capable of equilibrating the field, which is therefore viscously limited and scales as $\varepsilon^{1/2}$ in the asymptotic limit. Beyond D_x the inclusion of the ageostrophic nonlinearities once again equilibrates the field, and the data presented here would suggest that the average amplitude in some sense is independent of ε, but that the details of the evolution are not.

One might conjecture that beyond D_x a Taylor state exists, but is unstable. Since

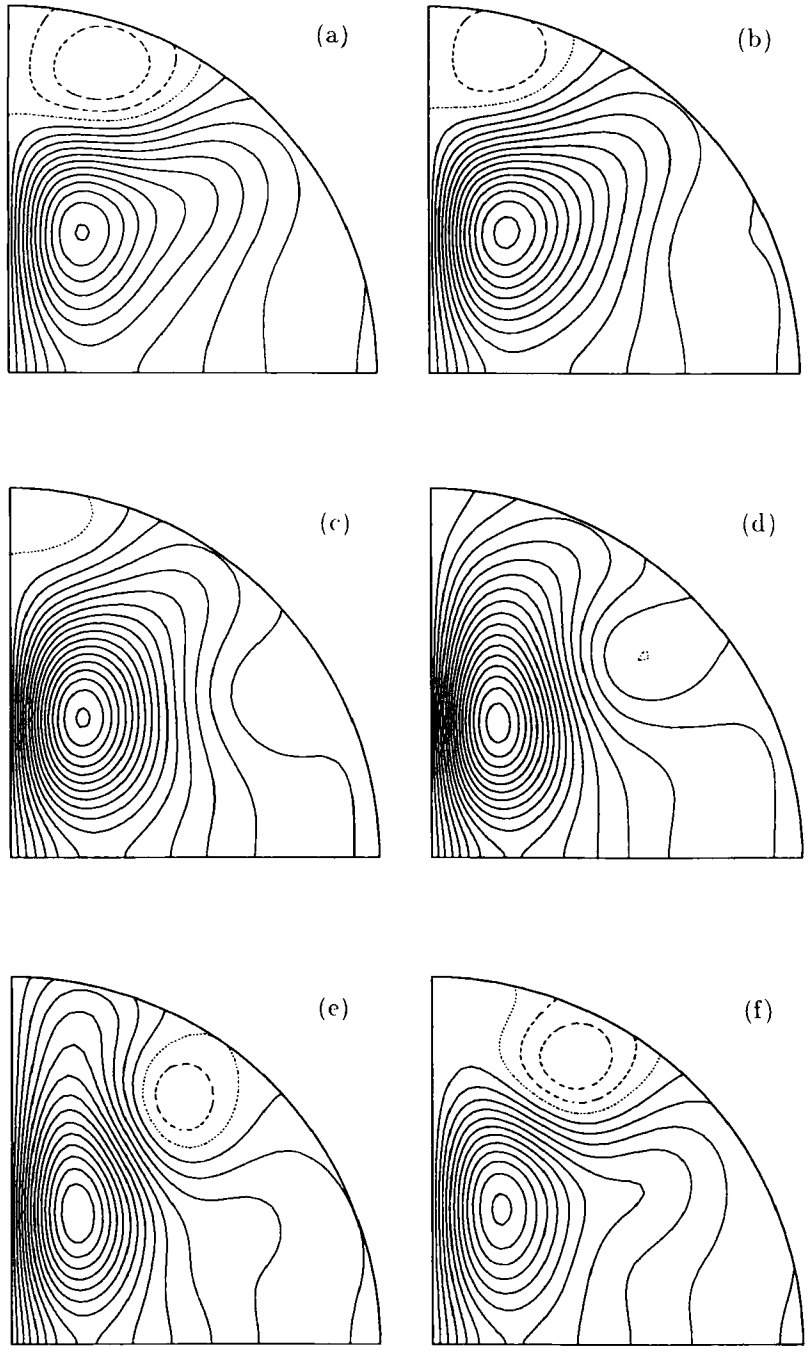

Figure 15 The spatial structure of A for $D = 20000$ through one period. (a) $t = (1/6)T$, (b) $t = (2/6)T$, (c) $t = (3/6)T$, (d) $t = (4/6)T$, (e) $t = (5/6)T$, (f) $t = (6/6)T$.

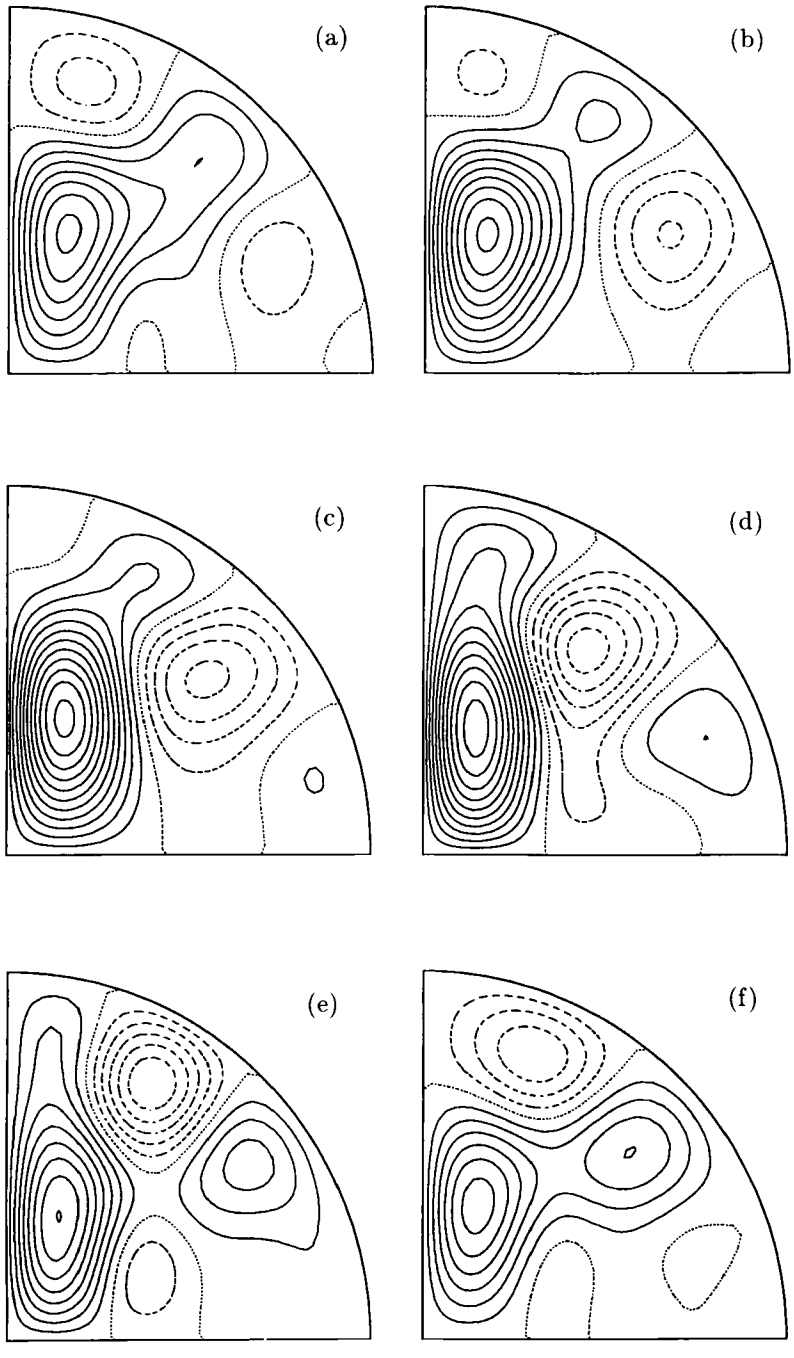

Figure 16 The spatial structure of B for $D=20000$ through one period. (a) $t=(1/6)T$, (b) $t=(2/6)T$, (c) $t=(3/6)T$, (d) $t=(4/6)T$, (e) $t=(5/6)T$, (f) $t=(6/6)T$.

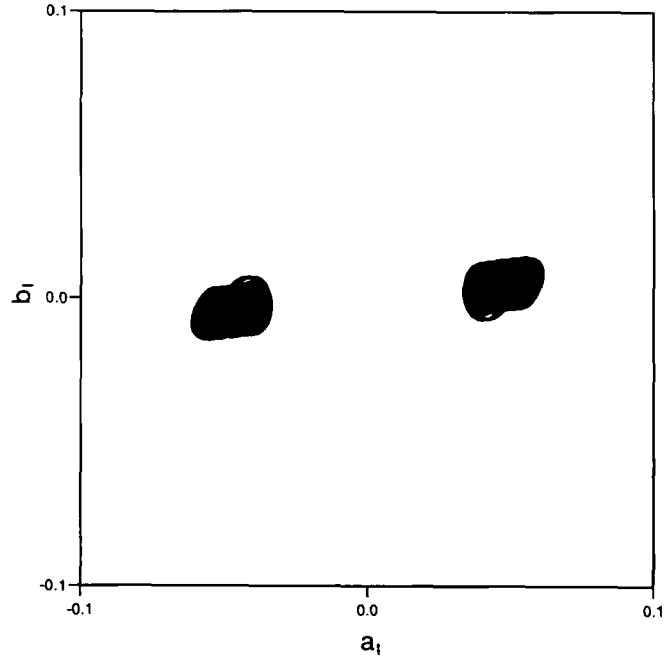

Figure 17 Two quasi-periodic trajectories in phase space for $D = 23000$, $\varepsilon^{-1} = 100$.

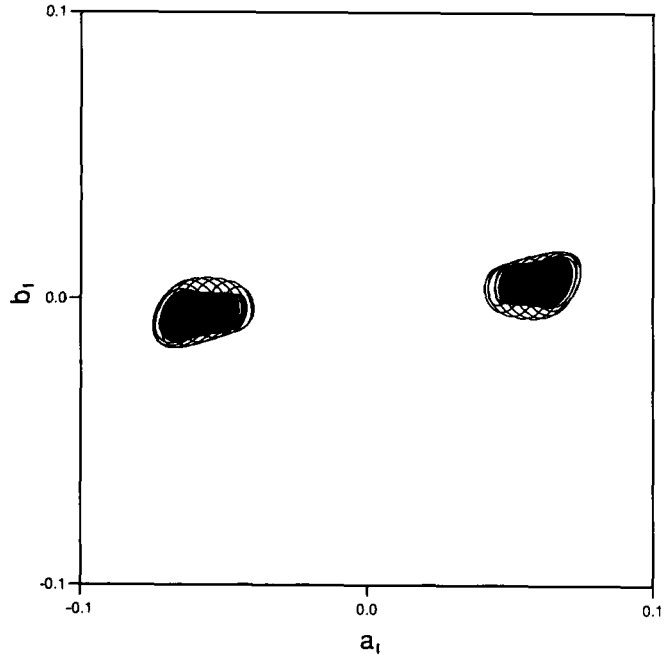

Figure 18 Two quasi-periodic trajectories in phase space for $D = 23200$, $\varepsilon^{-1} = 200$.

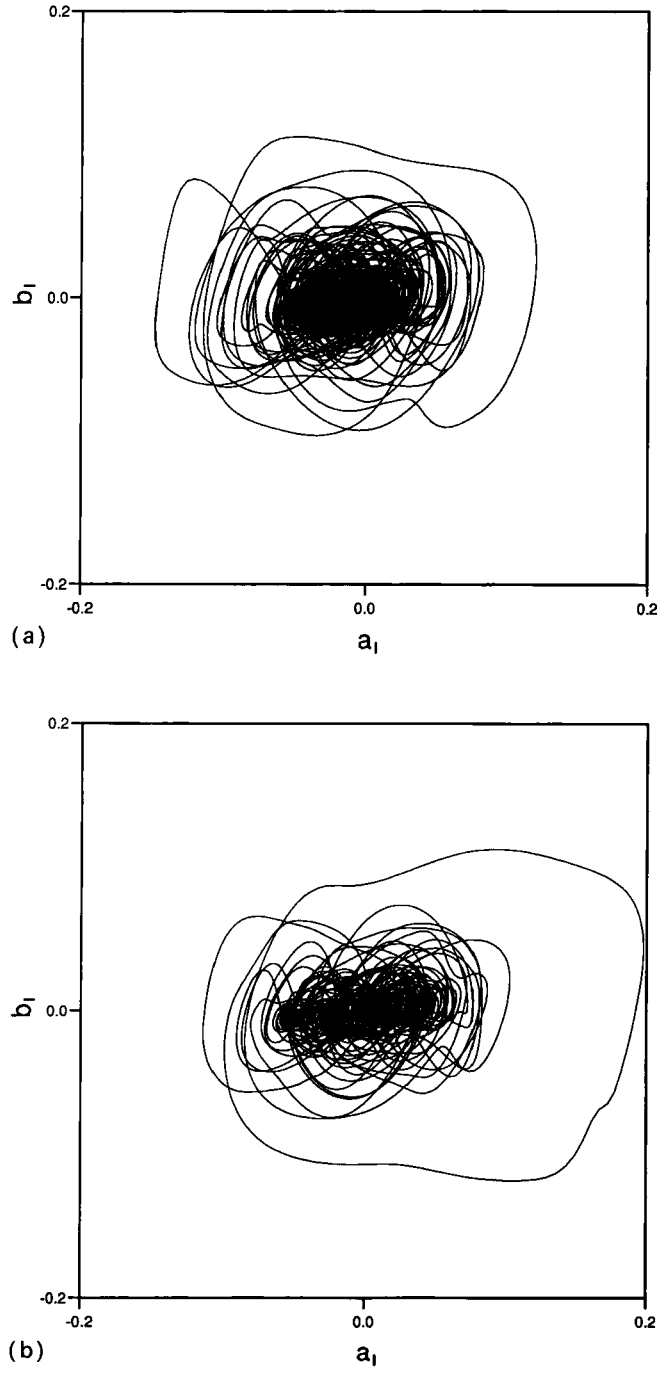

Figure 19 Two chaotic trajectories for $D=25000$, (a) $\varepsilon^{-1}=100$, (b) $\varepsilon^{-1}=200$. Each trajectory was run for 10 units of time, after allowing for the decay of transients.

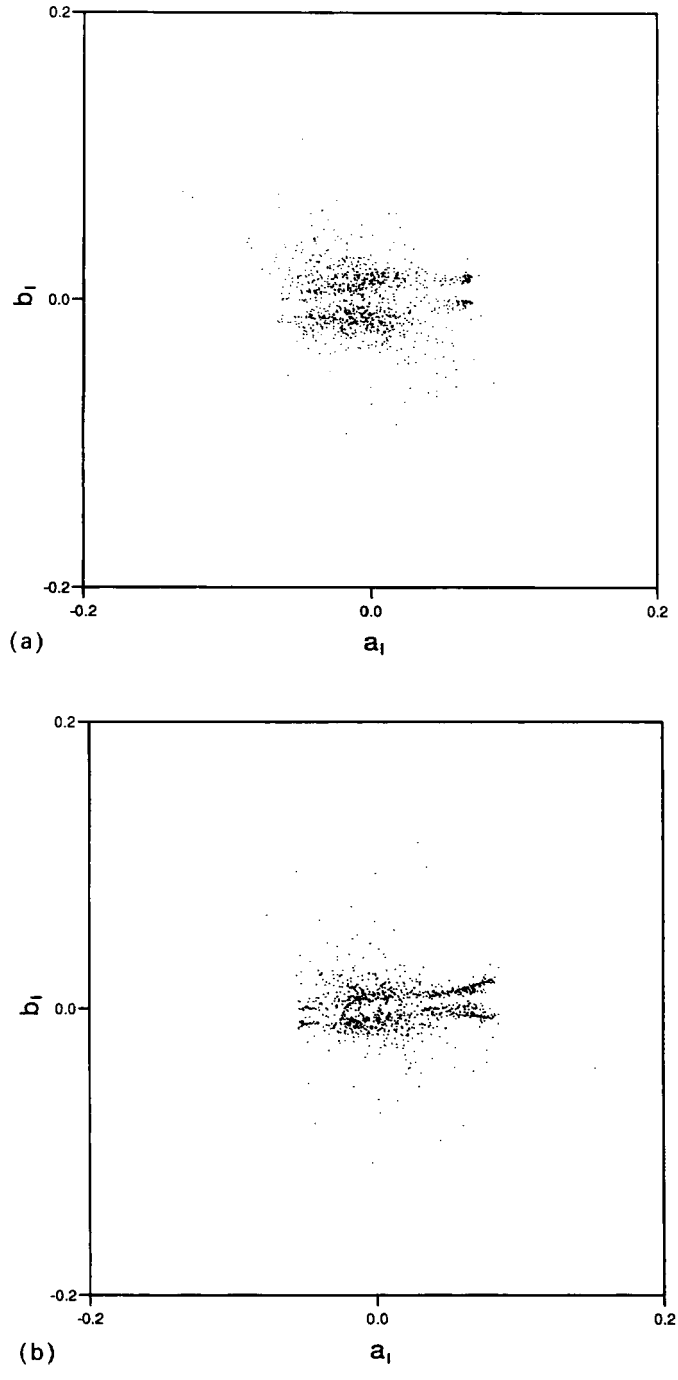

Figure 20 Two Poincaré sections for $D = 25000$. (a) $\varepsilon^{-1} = 100$, (b) $\varepsilon^{-1} = 200$. Each trajectory was run for 30 units of time, after allowing for the decay of transients.

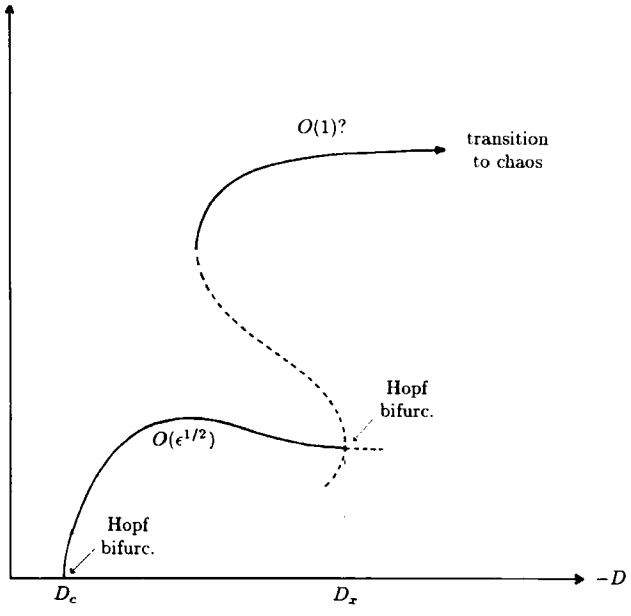

(a)

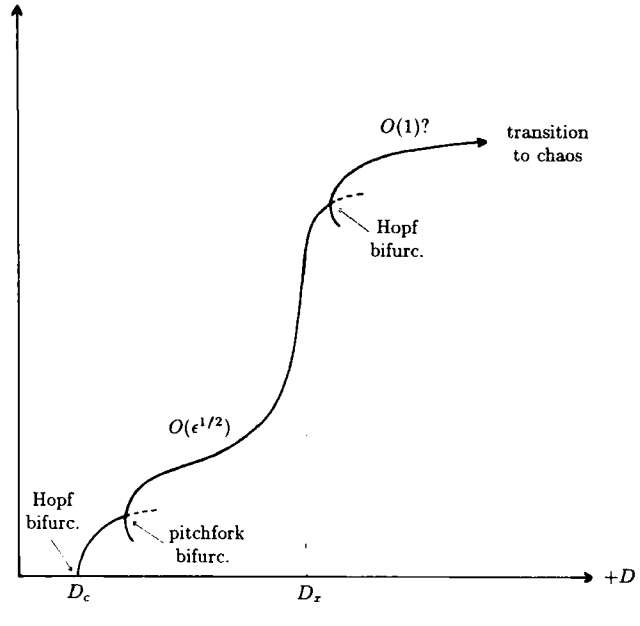

(b)

Figure 21 The postulated bifurcation diagram, showing some arbitrary measure of the amplitude as a function of negative (a) and positive (b) dynamo numbers.

the viscously limited regime is known to be unstable beyond D_x, one would then anticipate the temporal evolution to be a complicated interaction of the two. Previous models of Taylor's constraint in the limit of small viscosity have tended to follow either the Malkus and Proctor (1975) equilibration, or the Braginsky (1975, 1978) model-Z equilibration. It is not known whether the geodynamo is currently in a viscously limited state (unlikely), a Taylor state, or a model-Z state, but the possibility should not be overlooked that at different times it might be in different equilibration regimes. The dominant dipole state could, for instance, be a Taylor state (or a model-Z state) that eventually becomes unstable and collapses to a viscously limited state, which then regenerates a new dominant dipole (of possibly reversed polarity).

The second point raised by this work concerns the relevance of $\alpha\omega$ solutions to the geodynamo. The solutions presented here are not particularly reminiscent of the geodynamo. Unfortunately, they do appear to be the typical behaviour for most choices of α and ω. This would suggest one of two possibilities:

Firstly, one could suppose that the geodynamo operates with some very special choices of α and ω. Indeed, model-Z seems to depend on picking just the right choices. However, in the absence of a clearer theoretical understanding of the small-scale convective motions that generate α, such an approach is somewhat unsatisfactory. It seems unlikely that the α and ω of the geodynamo are time-independent, and even more unlikely that they have a simple spatial structure.

Alternatively, the failure of more typical $\alpha\omega$ solutions to model the geodynamo may indicate that the pure $\alpha\omega$ limit is not appropriate. We found that to get dynamo action at all the product of the nondimensionalized α and ω effects had to be at least O(1000). If one considers geophysical estimates of the dimensional quantities involved, one finds that the ω-effect can account for at most a factor of O(100), and so the α-effect must account for at least a factor of O(10). Thus, the ratio of α to ω in (2.5b) is at least O(0.1), sufficiently large that it may not be negligible. Indeed, an α of O(10) is sufficiently large to drive an α^2-dynamo, as in (2.1), without any ω at all.

It may thus be more appropriate to consider $\alpha^2\omega$-dynamos, intermediate between α^2 and $\alpha\omega$. The behaviour of such solutions in the limit of vanishing viscosity could turn out to be more relevant to the geodynamo. Braginsky and Roberts (1987) close with the (under)statement "We feel that some aspects of $\varepsilon\to 0$ asymptotics are still only partially understood." We can only concur.

Acknowledgements

This work was funded by the Science and Engineering Research Council under grant number GR/E93251.

References

Barenghi, C. F. and Jones, C. A., "Nonlinear planetary dynamos in a rotating spherical shell," *Geophys. Astrophys. Fluid Dynam.* **60,** 211–243 (1991).

Braginsky, S. I., "Nearly axially symmetric model of the hydromagnetic dynamo of the Earth, I," *Geomagn. Aeron.* **15,** 122–128 (1975).

Braginsky, S. I., "Nearly axially symmetric model of the hydromagnetic dynamo of the Earth, II," *Geomagn. Aeron.* **18,** 225–231 (1978).

Braginsky, S. I. and Roberts, P. H., "A model-Z geodynamo," *Geophys. Astrophys. Fluid Dynam.* **38,** 327–349 (1987).

Hollerbach, R., "Parity coupling in α^2-dynamos," *Geophys. Astrophys. Fluid Dynam.* **60,** 245–260 (1991).

Hollerbach, R. and Ierley, G. R., "A modal α^2-dynamo in the limit of asymptotically small viscosity," *Geophys. Astrophys. Fluid Dynam.* **56,** 133–158 (1991).

Jones, C. A. and Wallace, S. G., "Periodic, chaotic, and steady solutions in $\alpha\omega$-dynamos," in this Special Issue **67**, 37–64 (1992).

Malkus, W. V. R. and Proctor, M. R. E., "The macrodynamics of α-effect dynamos in rotating fluids," *J. Fluid Mech.* **67,** 417–443 (1975).

Roberts, P. H., "Kinematic dynamo models," *Phil. Trans. R. Soc. Lond.* A **272,** 663–698 (1972).